Available online at www.sciencedirect.com
ScienceDirect
Surface Science 602 (2008) 268–275
SURFACE SCIENCE
www.elsevier.com/locate/susc

# DFT characterization of coverage dependent molecular water adsorption modes on α-$Al_2O_3$(0001)

Víctor A. Ranea [a,c], William F. Schneider [b,*], Ian Carmichael [a]

[a] *Radiation Laboratory, University of Notre Dame, Notre Dame, IN 46556, United States*
[b] *Department of Chemical and Biomolecular Engineering, 182 Fitzpatrick Hall, University of Notre Dame, Notre Dame, IN 46556, United States*
[c] *Instituto de Investigaciones Físico-Químicas Teóricas y Aplicadas (CONICET), Suc. 4, C.C. 16 (1900) La Plata, Fac. de Cs. Exactas, Univ. Nac. La Plata, Argentina*

Received 29 May 2007; accepted for publication 10 October 2007
Available online 26 October 2007

**Abstract**

*Ab initio* density functional theory was used to investigate the stable and metastable states of adsorbed molecular water on the α-$Al_2O_3$(0001) surface as a function of coverage. The atoms of the dry surface undergo pronounced inward relaxations with respect to their bulk positions. At low coverages ($\Theta \leqslant 0.5$) water adsorbs nearly parallel to the surface plane, with an O atom atop a surface Al. The adsorption is mainly due to the donation from water lone pairs into vacant p orbital of surface Al, drawing the surface Al outward. With increasing coverage, water adsorption atop Al competes with an alternative configuration with water bound through H to surface oxygen. These two competing modes generate a variety of distinct but nearly isoenergetic adsorption modes that terminate in a hexagonal, ice-like layer at a coverage of two water molecules per surface Al. The binding energy per water molecule is maximized in the two limits of coverage, but deviates from this extreme only slightly at intermediate coverages. At no coverage is the water binding great enough to overcome the energetic preference for water to dissociatively adsorb.


*Keywords:* Density functional calculations; Adsorption; Aluminium oxide; Water

## 1. Introduction

The interaction of water with metal oxide surfaces has wide importance in subjects as diverse as heterogeneous catalysis and photocatalysis, corrosion, and environmental chemistry. Further, the ability of water to adsorb molecularly and dissociatively, to create a variety of surface functional groups, and to form strong hydrogen bond networks all contribute to a surface chemistry that is rich, complex, and not fully understood [1,2].

Because it is crystallographically well-defined, easily prepared, and chemically interesting, the Al-terminated α-$Al_2O_3$(0001) surface is a widely studied model for water reactions with metal oxide surfaces. A variety of experimental methods have been used to characterize this surface in the presence of water, including photoelectron [3,4] and vibrational [5] spectroscopies, LEED [6–9], thermal and laser-induced desorption [10], AFM [11,12] and dynamic-mode SFM [13], and surface-sensitive x-ray diffraction methods [8,14]. The general picture that emerges is of water adsorbing to the surface in both molecular and dissociative forms and of surface coverage states that depend strongly on environmental and preparative conditions. Molecular water tends to be more readily removed, for instance by vacuum outgassing at elevated temperatures, but surface hydroxyl groups are found to be robust even to 1000 °C ([15] and references within).

Computational studies are in good agreement with this description: a single water is found to chemisorb at exposed Lewis acidic Al sites of the (0001) surface and to

* Corresponding author. Tel.: +1 574 631 8754; fax: +1 574 631 8366.
*E-mail address:* wschneider@nd.edu (W.F. Schneider).

0039-6028/$ - see front matter © 2007 Elsevier B.V. All rights reserved.
doi:10.1016/j.susc.2007.10.029

exothermically dissociate with minimal activation energy across Al–$O_s$ bonds: [16–20]

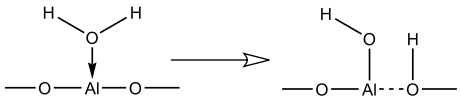

First-principles molecular dynamics [16,17] and thermodynamics [21–23] simulations predict a full hydroxylated surface to be the equilibrium termination at higher exposures to water, consistent with experimental equilibrium observations [14]. Between these two limiting cases of an isolated chemisorbed water molecule and a fully developed, hydroxylated surface, molecular-level details are more scant. Such details are important for describing the kinetics of hydroxylation, the intermediate surface species that are formed, and in general the surface chemistry of α-alumina in the presence of adsorbates in combination with water.

In this work we use plane-wave, supercell DFT simulations to take a first step in this direction, to examine the coverage-dependence of molecular water adsorption on α-$Al_2O_3$(0001) up to 2 ML (two water molecules per $(1 \times 1)$ surface unit cell). We systematically examine a large number of alternative adsorption configurations at coverages from 1/4 to 2 ML, in 1/4 ML increments, to ensure that representative minima are identified. We show that a variety of metastable molecular water adsorption states are possible, derived from two types of water-surface interactions combined with water–water hydrogen bonding. Surprisingly, these interactions tend to combine in such a way to provide a nearly constant adsorption energy as a function of coverage, up to a nominally two monolayer (2 ML = two $H_2O$/surface Al) water coverage.

## 2. Methodology

First-principles total energy calculations were performed within the supercell DFT framework using the Vienna *Ab initio* Simulation Package (VASP) [24]. Electon exchange and correlation were treated within the generalized gradient approximation (GGA) in the Perdew-Wang 91 form [25]. The Kohn-Sham equations were solved using the projector augmented wave (PAW) approach for describing electronic core states [26] and a plane-wave basis set truncated at a kinetic energy cut-off of 400 eV. The Brillouin zone of the hexagonal supercell was sampled with a Γ-point centered $(3 \times 3 \times 1)$ mesh, resulting in a set of five symmetry-unique $\boldsymbol{k}$-points. No symmetrization was applied in the surface calculations. The self-consistent-field was considered converged when the difference in total energy between iterations was less than $10^{-4}$ eV, and ionic relaxations were considered converged when the forces on ions were less than 0.03 eV/Å.

The α-$Al_2O_3$ bulk structure can be described as a slightly distorted hexagonal close packing of O atoms with Al atoms occupying two-thirds of the octahedral interstices [27]. Within the approximations used here we calculate the bulk lattice constants to be $a = 4.806$ and $c = 13.119$ Å, respectively. These computed values exceed the experimentally observed lattice constants [28,29] by approximately 1%, as is typical for the GGA. The calculated lattice constants are used in all reported calculations.

As described below, the stoichiometric α-$Al_2O_3$(0001) surface was modeled by a twelve-ion-layer-thick slab. The seven upper-most layers and adsorbed water molecules were allowed to relax freely while the five bottom-most layers were kept fixed in their ideal bulk positions. The slabs are separated by a vacuum region of 18 Å to minimize spurious interactions between periodic images. A $(2 \times 2)$ surface supercell ($Al_{32}O_{48}$) was used to study the adsorption of one (0.25 ML) up to eight (2 ML) water molecules.

To analyze electronic effects in the adsorption process, partial density of states calculations were performed for a single adsorbed $H_2O$. The total density of states was decomposed into atomic contributions by integrating the atomic charge density within a radius of 1.402, 0.820 and 0.370 Å about Al, O and H atoms, respectively. Partial density of states were obtained by projecting onto spherical harmonics centered on the atoms. Vacuum energies were estimated from the planar averaged potentials in the middle of the vacuum regions of the slabs and molecules, and the DOS aligned to this vacuum energy.

## 3. Results and discussions

### 3.1. The α-$Al_2O_3$(0001) surface

In the [0001] direction, bulk α-$Al_2O_3$ can be described in terms of alternating O atom layers and Al atom bilayers (Fig. 1), with three times as many O as Al per layer. The ideal bulk spacing between O and Al layers is 0.85 Å and between Al layers is 0.49 Å. This layer structure implies three possible surface terminations: Al–$O_s$–Al–, $O_s$–Al–Al– and Al–Al–$O_s$– (Here $O_s$ refers to O atoms of the surface, to distinguish from water $O_w$). In agreement with previous reports [6,9,13,30–32], we find the non-polar Al–$O_s$–Al– termination (Fig. 1) to be lowest in energy and consider $H_2O$ adsorption only on this surface. In a set of calculations on an 18-layer-thick slab (6 O and 12 Al layers), the surface energy is well converged beyond relaxation of the topmost five layers and the displacement of ions from their ideal bulk locations is less than 1% beyond relaxation of seven layers. Further, the adsorption geometry and energy of a single water molecule in a $(1 \times 1)$ surface cell is identical to within <0.01 eV and 0.01 Å on slabs containing 12, 15, and 18 ion layers, i.e., to within the precision of the DFT calculations. Based on these results, we explore a wider range of water adsorption states using a 12 layer slab with 7 free layers (Fig. 1).

The calculated interlayer spacings are 0.10, 0.88, 0.27, 1.02, 0.89, 0.47 and 0.84 Å, in good agreement with previous reports [33,34]. In agreement with LEED analysis [6],

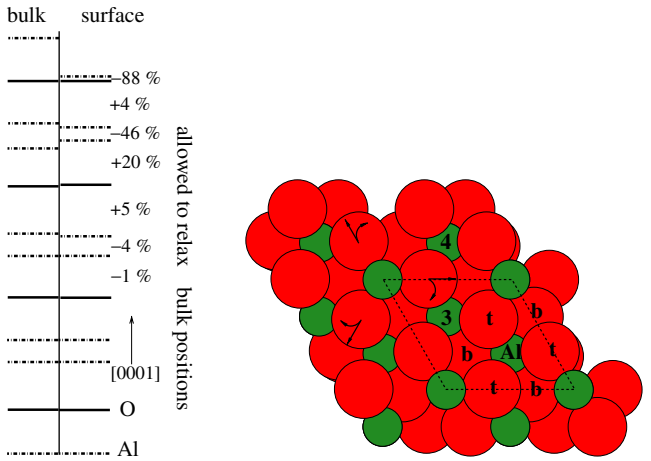


Fig. 1. Side and top views of relaxed α-$Al_2O_3$(0001)-(2 × 2) supercell. Side view indicates vertical relaxation of Al (dashed) and O (solid) layers relative to bulk locations. Medium green and large red circles represent Al and $O_s$ atoms, respectively in top view. Arrows indicate the rotation and lateral relaxation of $O_s$ about atop Al. Numbers identify Al layers and letters identify top (t) and bottom (b) vertices of the $AlO_6$ octahedron. 1 × 1 primitive cell indicated with dashed lines. (For interpretation of the references to colour in this figure legend, the reader is referred to the web version of this article.)

relaxed Al atoms remain in hexagonal locations but experience large vertical relaxations into the plane of the first $O_s$ layer in response to loss of O coordination. The calculated separation of 0.10 Å between the top two layers is slightly less than the 0.3 ± 0.1 Å range obtained with LEED [6]. In response to this Al relaxation, the second layer $O_s$ atoms relax laterally and rotate about the surface normal (Fig. 1) and the Al–$O_s$ bond lengths decrease from 1.87 to 1.70 Å (−9.1%), reflecting an increase in Al–$O_s$ bonding.

### 3.2. Molecular water adsorption on the α-$Al_2O_3$(0001) surface

We now consider the adsorption of successive water molecules at the α-$Al_2O_3$(0001) surface. As we show below, water can bind with the surface through Al–$OH_2$ and $O_s$–HOH interactions and, at increasing coverages, through interadsorbate hydrogen bonding. At 2 ML saturation the surface is found to form a hexagonal overlayer similar to the "bilayer" structure familiar to water adsorption on metal surfaces [1,35,36] but with little vertical separation between the O atoms of water. This saturated surface includes two water molecules per surface Al, or 8 waters per 2 × 2 supercell. We define this coverage as 2 ML and report other coverages relative to this value. Table 1 summarizes key geometric parameters.

To separate the effects of water-surface and water-water interactions, we distinguish between the total binding energy $E_{bind}$ between the surface and $n$ gas-phase water:

$$E_{bind} = E_{tot}(nH_2O/\alpha\text{-}Al_2O_3(0001)) - n \cdot E_{tot}(H_2O) - E_{tot}(\alpha\text{-}Al_2O_3(0001))$$

Table 1
Comparison of surface relaxations as a function of water coverage, including the distance between the $O_w$ and the atop Al atom, $D$, the change in the $z$ coordinate(s) of these "occupied" atop Al atom(s) ($\Delta_z$ atop) and of "unoccupied" Al atoms ($\Delta_z$bare)

| Θ (ML) | $D$ (Å) | $\Delta_z$atop (Å) | $\Delta_z$bare (Å) |
|---|---|---|---|
| 0.25 | 1.96 | +0.29 | −0.08 |
| 0.50 | 1.98 (2) | +0.28 (2) | −0.21 |
| 0.75 | 1.91, 1.94 | +0.34 (2) | −0.15, −0.23 |
| 1.00 | 1.88 (2) | +0.39 (2) | −0.28, −0.30 |
| 1.25 | 1.90 (2), 1.99 | +0.35 (2), +0.22 | −0.46 |
| 1.50 | 1.90, 1.93 (2) | +0.32, +0.33, +0.36 | −0.50 |
| 1.75 | 1.88, 1.91 (2) | +0.36 (3) | −0.55 |
| 2.00 | 1.93 (4) | +0.29 (4) | |

and the energy $E_{sep}$ to rigidly separate the partially or fully developed water overlayer ($n \cdot H_2O$) from the surface:

$$E_{sep} = E_{tot}(nH_2O/\alpha\text{-}Al_2O_3(0001)) - E_{tot}(n \cdot H_2O) - E_{tot}(\alpha\text{-}Al_2O_3(0001))$$

By this convention a negative separation energy corresponds to exothermic reaction. The difference between $E_{bind}$ and $E_{sep}$ reflects the contribution of interadsorbate bonding to the overall surface bonding.

#### 3.2.1. Isolated water adsorption

Molecular adsorption of a single, isolated water within the 2 × 2 supercell (corresponding to a surface density of $1.25 \times 10^{14}$ molecules $cm^{-2}$) occurs exclusively through water oxygen ($O_w$) to a surface Al (Fig. 2) with a binding energy of −1.14 eV. This value is ≈0.1 eV more exothermic than previous supercell [16] and embedded cluster DFT results [19]. We find the molecular adsorbed state to be unstable by 0.43 eV with respect to water dissociated to OH and H on neighbor surface Al and O.

As shown in Fig. 2, molecular water adsorbs approximately parallel to the surface, vertically drawing up the Al ion by 0.29 Å. The remaining three surface Al atoms relax downward by 0.08 Å. The three nearest neighbor $O_s$ are also drawn up and shifted toward the Al atom to maintain Al–$O_s$ bond lengths of about 1.7 Å. The Al–$O_w$ bond

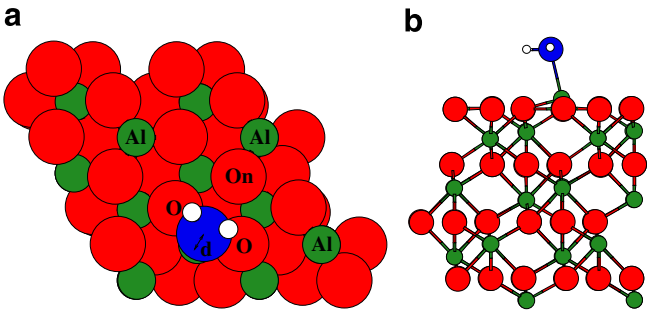


Fig. 2. Top and side views of isolated molecular water adsorption. Medium green, large red, large dark blue and small white circles correspond to Al, $O_s$, $O_w$ and H atoms, respectively. (For interpretation of the references in colour in this figure legend, the reader is referred to the web version of this article.)

length is decidedly longer, 1.96 Å, reflecting the relative weakness of this dative bond. The water molecule is minimally perturbed by adsorption. The importance of secondary interactions between water hydrogen and the surface oxygen is shown by the $d = 0.54$ Å lateral displacement from atop Al, resulting in separations between H atoms and nearest-neighbor $O_s$ of 2.33 and 2.56 Å. By comparison, rotating water such that one O–H bond points towards $O_n$ of Fig. 2 reduces the absolute binding energy by ≈0.02 eV. Constraining the water molecule to sit perpendicular to the oxide surface further decreases the binding energy to 0.98 eV. In agreement, experimental results indicate the isolated species are adsorbed with oxygen ends towards the surface $Al^{3+}$ cations. High resolution x-ray photoelectron spectroscopy of ultra-thin alumina films grown on NiAl(1 1 0) show evidence of only molecular water species at low-coverages [37].

The adsorbate-surface interaction is mediated by donation from Lewis basic water "lone pairs" into vacant, Lewis acidic surface orbitals [1]. The primary interactions are between the $1b_1$ and $3a_1$ molecular orbitals (MOs) of the water molecule with the empty orbitals of the Al atom (Fig. 3). The left side of Fig. 3 shows a general stabilization of the two lone pair water levels upon adsorption and in particular the appearance of a sharp bonding feature at low energy, corresponding to donation from these $O_w$ states into formerly vacant, hybridized Al $3p_z$ and 3s states (right). A corresponding antibonding level is pushed to high energy.

*3.2.2. Higher water coverages and lateral interaction effects*

Two distinct adsorption configurations can be accessed upon addition of a second water molecule to the $(2 \times 2)$ supercell (0.5 ML coverage). Most favored is adsorption at one of the vacant Al sites (Fig. 4) in a configuration similar to the 0.25 ML water case above. Rotation of the water about a surface normal produces at least two different surface orientations with binding energies of −2.23 (Fig. 4a) and −2.21 eV (Fig. 4b), almost exactly twice that of isolated molecular adsorption. The separation energies in both cases are −2.19 eV. Water–water interactions thus contribute somewhat less than 0.05 eV to the overall binding, so that the "intrinsic" water-surface interaction is slightly reduced relative to the 0.25 ML case. Consistent with this, the Al–$O_w$ bond distances are increased 0.02 Å relative to isolated adsorption, to 1.98 Å, while the internal water structures are unchanged. Also consistent with the 0.25 ML case, the Al atom adsorption sites are drawn up while the unoccupied Al sites relax downward below adjact $O_s$ by 0.1 Å. The entire second $O_s$ atoms layer is depressed by 0.02 Å.

Competing with these adsorption configurations are ones in which the second molecule is hydrogen bonded to the first as well as to the surface. This latter molecule acts both as a lone-pair donor to the water and an H-donor to surface oxygen (Fig. 5). A single water in this hydrogen bonding configuration relaxes spontaneously to an atop Al site, so the existence of this configuration is a direct

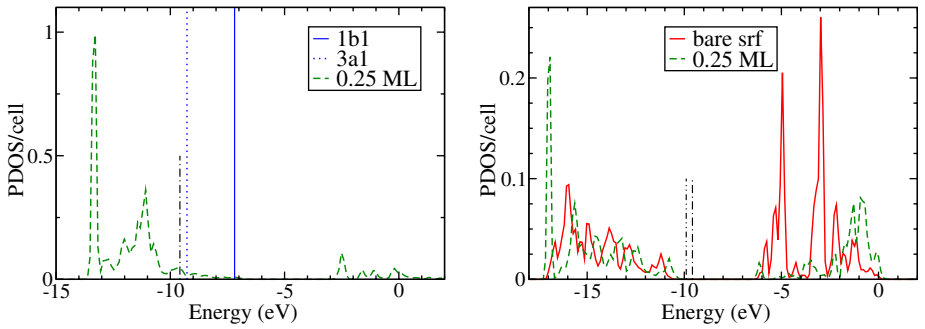


Fig. 3. (Left) Comparison of highest occupied MOs of an isolated water molecule (solid and dashed lines) with the *s* and *p* projected partial density of states (PDOS) of adsorbed water oxygen $O_w$. (Right) Comparison of Al 3s and $3p_z$ projected PDOS before and after water adsorption. Black dot–dot–dashed and dot–dashed lines indicate highest occupied states before and after adsorption, respectively.

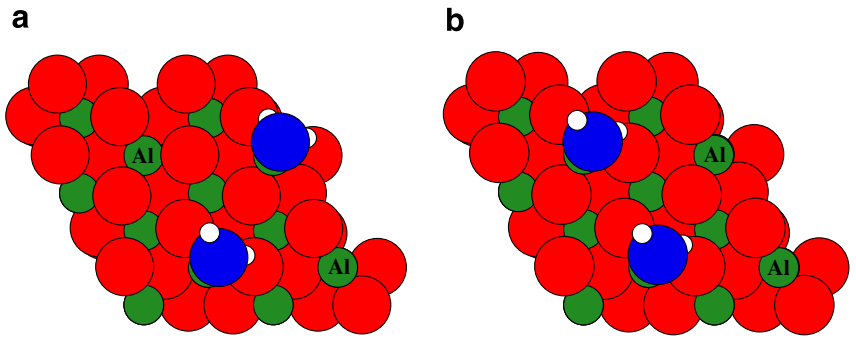


Fig. 4. Top views of most favorable water adsorption configurations at 0.5 ML coverage. Marked are the empty Al atoms of the outermost layer.

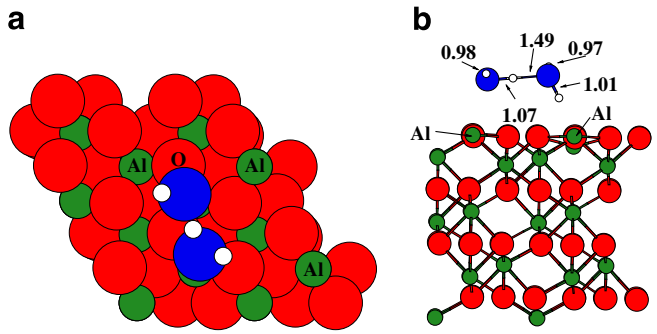


Fig. 5. Top (a) and side (b) views of two-water cluster. Marked with O is the HOH-bound $O_s$.

consequence of water–water interactions. This complex cannot be described as a simple water dimer adsorbed to the surface, however: to accommodate the alumina lattice, the hydrogen bond distance (1.49 Å) is significantly compressed relative to an unconstrained gas-phase dimer (1.88 Å). As a result, the binding and separation energies of this configuration are a nearly identical −2.03 eV. Reorientation of the hydrogen-bonded water molecule as an H donor to both $O_w$ and $O_s$ reduces the binding energy to −1.50 eV.

These results can be contrasted to the adsorption of water on a Pd{1 1 1} metal surface [38,39]. The interaction of a water molecule with a metal surface is weaker than the H-bond between two water molecules, and because of the low barrier to diffusion, water molecules will cluster even at low temperatures [38]. While a single water adsorbs atop Pd, a second water prefers to hydrogen bond to the first, with minimal direct interaction with the metal surface [39].

At a coverage of $\Theta = 0.75$ ML, the balance between adsorption atop surface Al and through hydrogen-bonding to $O_s$ becomes even closer (Fig. 6). In addition, depending on starting configuration, some of the water adsorbate structures relaxed spontaneously to dissociated states, reflecting the low barrier to water-assisted water dissociation [16]. Three isolated molecular water adsorb atop surface Al with a binding energy of −3.17 eV (Fig. 6c). Following trends noted above, adsorption draws up occupied Al sites by 0.24 Å while the vacant Al atom is drawn down by 0.29 Å, to a position that is actually below the $O_s$ layer by 0.2 Å.

Slightly lower in energy is an adsorption configuration with two water atop Al and the third water inserted as a hydrogen bonding bridge. The exact binding energy depends on the orientation of the bridging water; as shown in Fig. 6 the most favorable of these involves lone pair donation to both Al atop waters as well as H-donation towards surface oxygen, with a calculated binding energy of −3.26 eV (Fig. 6a and b). Reorientation to break one of the interwater hydrogen bonds costs approximately 0.2–0.3 eV, and converting a second atop Al water to a hydrogen bonding location (Fig. 6d) further decreases the binding energy to −2.79 eV.

As in the water dimer case above, the intermolecular hydrogen bond distances in the mixed 2 atop/1 HOH–$O_s$ bonded configuration are significantly compressed to accommodate binding to the alumina lattice. Thus, the separation energy of this configuration is actually more negative than the binding energy. The alumina surface acts as a template for adsorption of water clusters, dominating the interadsorbate interactions.

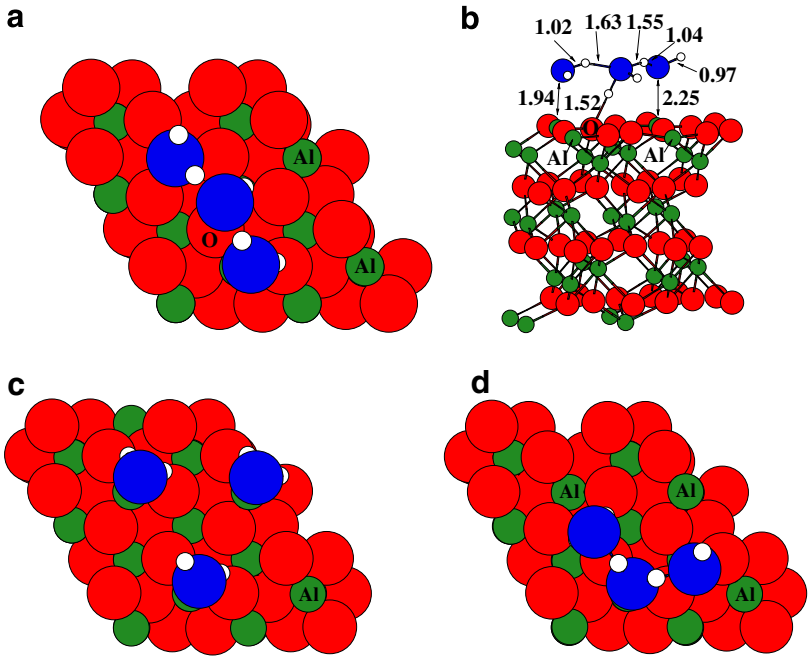


Fig. 6. Top and side views of the most stable three-water cluster (a and b) and competing isolated water (c) and cluster (d) configurations.

One water molecule per surface Al is often termed 1 ML coverage, although as we show below, within this DFT model it does not represent saturation coverage of the basal plane. At this coverage the most stable configurations involve some combination of Al-bound and hydrogen-bonded water molecules. In competition with these mixed configurations is one in which every surface Al adsorbs a water. The binding energy of this water-atop-Al surface is −1.00 eV per molecule, or 0.14 eV weaker than the low coverage value. Increasing surface strain induced by distortions of surface Al from their relaxed dry surface locations accounts for this decreasing average binding energy.

More stable by 0.12 eV per molecule (for a total binding energy of −4.48 eV) is a configuration in which half the molecules adsorb parallel to the surface atop Al atoms and the other half hydrogen bond to $O_s$ in such a way to form a one-dimensional water chain (Fig. 7a), bound by hydrogen bond donation from atop water into the lone pairs of HOH–$O_s$ water. This chain, although compressed, does contribute significantly to the stability of the configuration, as shown by the 1.41 eV positive difference between separation and binding energies. Breaking the chain, for instance as in a configuration with 3/4 of the water adsorbed atop Al and 1/4 H-bonded (Fig. 7b), costs approximately 0.2 eV in binding energy.

The addition of a fifth water molecule ($\Theta = 1.25$ ML) continues the development of the molecular net of adsorbed water molecules. The most strongly adsorbed configuration adds a water atop a vacant Al site to the 1 ML molecular water chain (Fig. 8). As the chain completely occupies the lone pairs of HOH–$O_s$ water, this additional water is connected to the chain via a relatively long hydrogen bond interaction. Additional waters add in such a way to build up a second water chain parallel to the first, and the successive binding energies are nearly constant.

Finally at eight water, or $\Theta = 2.00$ ML, the two parallel chains are completed, and these are bridged through longer (2.1 Å) hydrogen bonds to form a hexagonal network of waters similar in connectivity but different in vertical corrugation to hexagonal ice (Fig. 9). Here, half the water are bound parallel to the surface atop Al atoms and half are bound perpendicular to the surface through H-bonds to $O_s$ as well as via H-bonds to neighbor water. The individual water angles widen and bonds lengthen to accommodate binding to the alumina surface. The HOH–$O_s$ separation are a short 1.63 to 1.71 Å. The surface Al atoms rise to 0.40 Å above the $O_s$ plane, and the $O_s$ are drawn up 0.05 Å. Atoms further subsurface are largely unaffected by the presence of the molecular water layers. The binding and separation energies are −9.09 and −6.94 eV, respectively. Almost a quarter (≈24%) of the binding energy can thus be attributed to interactions among water molecules within the adsorbate layer.

Despite the fact that the two types of water comprising the bilayer bind to the alumina surface in different ways, their O atoms differ in height above the surface by only 0.13 Å, so that the resulting hexagonal "bilayer" is nearly uniform in thickness. Significant strain does remain within this hexagonal water layer. When isolated and allowed to relax absent the influence of the underlying alumina

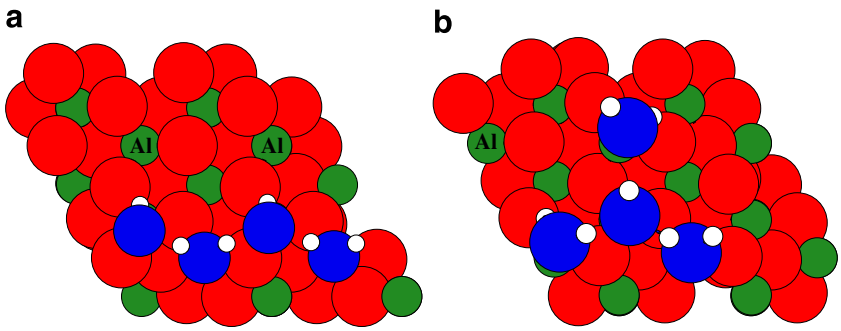


Fig. 7. Top views of the 1 ML one-dimensional water chain (a) and a less stable water cluster (b).

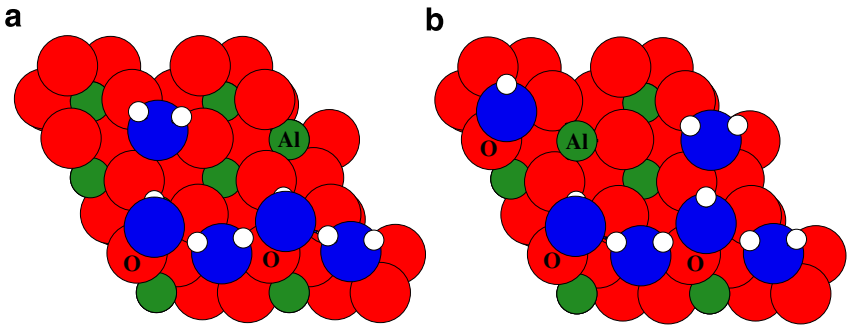


Fig. 8. Top views of five (a) and six (b) water molecules adsorbed per 2 × 2 supercell.

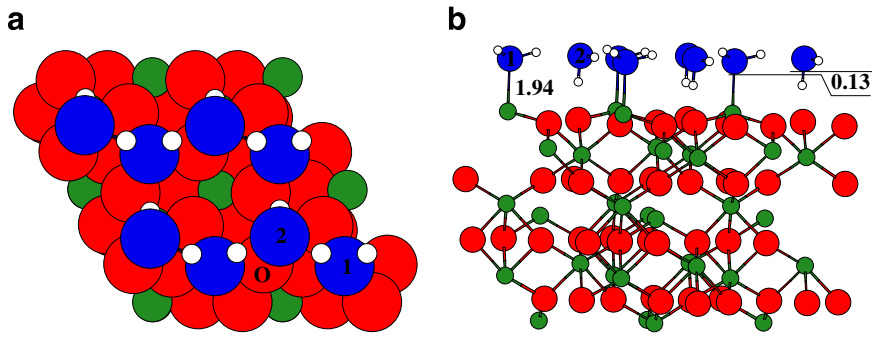


Fig. 9. Top (a) and (b) side views of 2 ML $H_2O$. $H_2O$ atop Al are marked with **1** and HOH-$O_s$ indicated with **2**. Distances in Å.

surface, the layer retains its basic topology, but it contracts laterally slightly and the two water types experience significant vertical relaxations, so that the distance between the planes of the two water rises to 0.64 Å. Further, the half of the water involved in direct hydrogen bonding to the surface reorient their H atoms away from the surface in an "H-up" conformation. Unlike water bilayers at metal surfaces [40,41], this reorientation is energetically costly in the presence of the alumina surface. Thus, the "bilayer" water bound to the α-$Al_2O_3$(0001) oxide surface is one influenced by strong and specific interactions with both surface cations and oxygen.

A comparison between binding energy per water molecule and separation energy per water molecule is made in Fig. 10. The binding energy is greatest in the two extremes of coverage examined here, 0.25 and 2.00 ML. Intermediate coverages are somewhat less strongly bound, but the differences are not great despite the fact that different types of binding sites are occupied across the series. The separation energy, in contrast, decreases in magnitude nearly uniformly across the series, reflecting an increasingly large contribution of intermolecular interactions that closely balance a decrease in adsorbate-surface binding at increasing coverage. Deviations from this trend at intermediate water coverages result from the appearance of direct water–water interactions at the 3-water (3/4 ML) coverage and the formation of a continuous water chain at the 4-water (1 ML) coverage. In undertaking this study we hypothesized, based on the stability of ice-like water layers on metal surfaces, that the combination of surface bonding and intermolecular interactions could be great enough to energetically stabilize a water overlayer against dissociative adsorption, possibly contributing to the observed existence of metastable molecular water on some alumina surfaces [37]. Such is apparently not the case on the α-$Al_2O_3$(0001) surface: the average binding energies are essentially constant with coverage and are approximately uniformly unstable to dissociation. Consideration of the structure, energetics, and kinetics of water dissociation vs. coverage is the topic of a separate report.

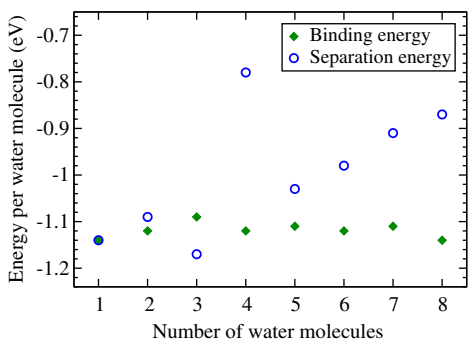


Fig. 10. Most stable bonding and corresponding separation energies per water molecule as a function of water content per 2 × 2 supercell.

## 4. Conclusions

The adsorption of water molecules on the α-$Al_2O_3$(0001) surface has been studied as a function of the coverage (Θ = 0.25 to 2.00 ML) using *ab initio* GGA, supercell methods. We identify two competing types of molecular adsorption, one with water bound through oxygen to surface Al and the other with water bound through hydrogen to surface O. The former predominates at low coverage, but at increasing water density, the opportunity to form additional hydrogen bonds between adsorbed waters makes occupancy of the second type of site competitive. The average binding energy is essentially constant up to a coverage of 2 ML, or two water per surface Al, at which a flat, hexagonal ice-like layer is completed.

## Acknowledgement

The research described herein was supported by the Office of Basic Energy Sciences of the US Department of Energy. This is contribution number NDRL-4729 from the Notre Dame Radiation Laboratory.

## References

[1] P.A. Thiel, T.E. Madey, Surf. Sci. Rep. 7 (1987) 211.
[2] M.A. Henderson, Surf. Sci. Rep. 46 (2002) 1.
[3] D.B. Almy, D.C. Foyt, J.M. White, J. Electron Spectroscopy 11 (1997) 129.
[4] P. Liu, T. Kendelewicz, G.E. Brown Jr., E.J. Nelson, S.A. Chambers, Surf. Sci. 417 (1998) 53.
[5] H.A. Al-Abadleh, V.H. Grassian, Langmuir 19 (2003) 341.
[6] J. Ahn, J.W. Rabalais, Surf. Sci. 388 (1997) 121.
[7] J. Toofan, P.R. Watson, Surf. Sci. 401 (1998) 162.

[8] G. Renaud, B. Villette, I. Vilfan, A. Bourret, Phys. Rev. Lett. 73 (1994) 1825.
[9] E.A. Soares, M.A. van Hove, C.F. Walters, K.F. McCarty, Phys. Rev. B 65 (2002) 195405.
[10] C.E. Nelson, J.W. Elam, M.A. Cameron, M.A. Tolbert, S.M. George, Surf. Sci. 416 (1998) 341.
[11] J.R. Heffelfinger, M.W. Bench, C.B. Carter, Surf. Sci. 370 (1997) L168.
[12] Y. Gan, G.V. Franks, J. Phys. Chem. B 109 (2005) 12474.
[13] C. Barth, M. Reichling, Nature 414 (2001) 54.
[14] P.J. Eng, T.P. Trainor, G.E. Brown Jr., G.A. Waychunas, M. Newville, S.R. Sutton, M.L. Rivers, Science 288 (2000) 1029.
[15] B.A. Hendriksen, D.R. Pearce, R. Rudham, J. Catal. 24 (1972) 82.
[16] K.C. Hass, W.F. Schneider, A. Curioni, W. Andreoni, Science 282 (1998) 265.
[17] K.C. Hass, W.F. Schneider, A. Curioni, W. Andreoni, J. Phys. Chem. B 104 (2000) 5527.
[18] J.M. Wittbrodt, W.L. Hase, H.B. Schlegel, J. Phys. Chem. B 102 (1998) 6539.
[19] V. Shapovalov, T.N. Truong, J. Phys. Chem. B 104 (2000) 9859.
[20] M.A. Nygren, D.H. Gay, D.R.A. Catlow, Surf. Sci. 380 (1997) 113.
[21] R. Di Felice, J.E. Northrup, Phys. Rev. B 60 (1999) R16287.
[22] X.-G. Wang, A. Chaka, M. Scheffler, Phys. Rev. Lett. 84 (2000) 3650.
[23] Z. Łodziana, J.K. Nørskov, P. Stoltze, J. Chem. Phys. 118 (2003) 11179.
[24] G. Kresse, J. Hafner, Phys. Rev. B 47 (1993) 558;
G. Kresse, J. Hafner, Phys. Rev. B 48 (1993) 13115;
G. Kresse, J. Hafner, Phys. Rev. B 49 (1994) 14251.
[25] J.P. Perdew, J.A. Chevary, S.H. Vosko, K.A. Jackson, M.R. Pederson, D.J. Singh, C. Fiolhais, Phys. Rev. B 46 (1992) 6671;
J.P. Perdew, J.A. Chevary, S.H. Vosko, K.A. Jackson, M.R. Pederson, D.J. Singh, C. Fiolhais, Phys. Rev. B 48 (1993) 4978;
J.P. Perdew, J.A. Chevary, S.H. Vosko, K.A. Jackson, M.R. Pederson, D.J. Singh, C. Fiolhais, Phys. Rev. B 45, 13244.
[26] P.E. Blöch, Phys. Rev. B 50 (1994) 17953;
G. Kresse, D. Joubert, Phys. Rev. B 59 (1999) 1758.
[27] R.W.G. Wyckoff, Crystal Structures II, second ed., Wiley, New York, 1964.
[28] J. Lewis, D. Schwarzenbach, H.D. Flack, Acta Cryst. A 38 (1982) 733.
[29] P. Thompson, D.E. Cox, J.B. Hastings, J. Appl. Cryst. 20 (1987) 79.
[30] J. Guo, D.E. Ellis, D.J. Lam, Phys. Rev. B 45 (1992) 13647.
[31] P.D. Tepesch, A.A. Quong, Phys. Stat. Sol. (b) 217 (2000) 377.
[32] C. Noguera, J. Phys.: Condens. Matter 12 (2000) R367.
[33] C. Verdozzi, D.R. Jennison, P.A. Schultz, M.P. Sears, Phys. Rev. Lett. 82 (1999) 799.
[34] C. Ruberto, Y. Yourdshahyan, B.I. Lundqvist, Phys. Rev. B 67 (2003) 195412.
[35] G. Held, D. Menzel, Surf. Sci. 316 (1994) 92.
[36] H. Ogasawara, B. Brena, D. Nordlund, M. Nyberg, A. Pelmenschikov, L.G.M. Patterson, A. Nilsson, Phys. Rev. Lett. 89 (2002) 276102.
[37] G. Tzvetkov, Y. Zubavichus, G. Koller, Th. Schmidt, C. Heske, E. Umbach, M. Grunze, M.G. Ramsey, F.P. Netzer, Surf. Sci. 543 (2003) 131.
[38] T. Mitsui, M.K. Rose, E. Fomin, D.F. Ogletree, M. Salmeron, Science 297 (2002) 1850.
[39] V.A. Ranea, A. Michaelides, R. Ramírez, P.L. de Andrés, J.A. Vergés, D.A. King, Phys. Rev. Lett. 92 (2004) 136104.
[40] A. Michaelides, A. Alavi, D.A. King, Phys. Rev. B 69 (2004) 113404.
[41] A. Michaelides, Appl. Phys. A 85 (2006) 415.